Supplement of Atmos. Chem. Phys., 19, 5973–5991, 2019
https://doi.org/10.5194/acp-19-5973-2019-supplement

Atmospheric Chemistry and Physics
Open Access
EGU

Supplement of

Impact of anthropogenic and biogenic sources on the seasonal variation in the molecular composition of urban organic aerosols: a field and laboratory study using ultra-high-resolution mass spectrometry

Kaspar R. Daellenbach et al.

Correspondence to: André S. H. Prévôt (andre.prevot@psi.ch) and Markus Kalberer (markus.kalberer@unibas.ch)

1 Measurement location

The measurement sites in central Europe are displayed in Fig. S1.

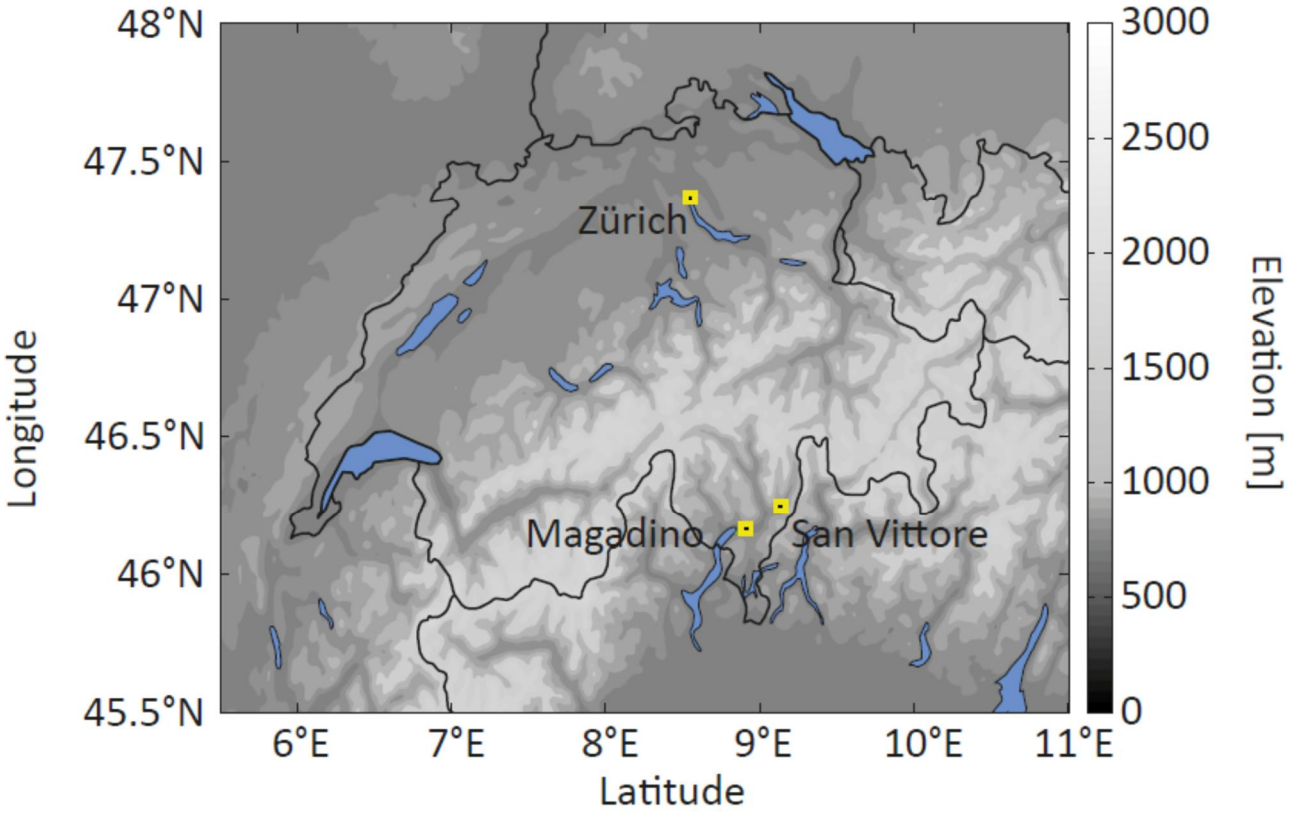

Figure S1: map of Switzerland and surrounding area with marked sampling locations.

2 Spatial and temporal variability of biogenic VOC emissions

Biogenic sesquiterpene and isoprene emissions normalized to biogenic monoterpene emissions are presented in Fig. S2 (as modelled in Jian et al., 2019).

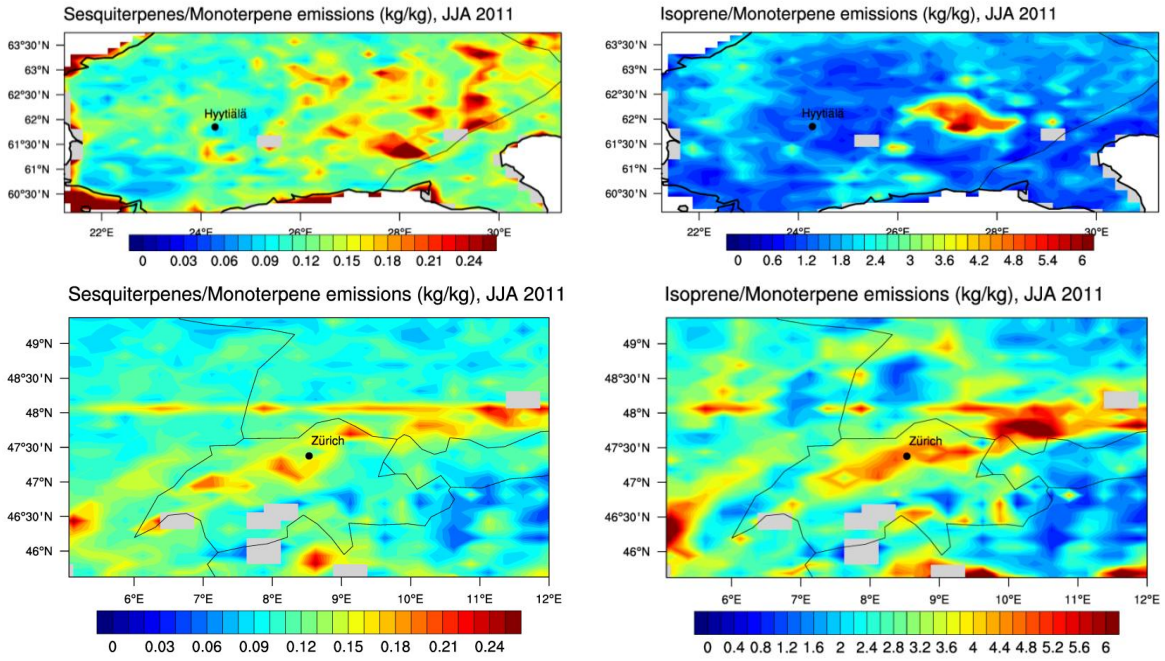

Figure S2: biogenic emissions of isoprene (ISO), monoterpene (MT), and sesquiterpenes (SQT) displayed as ratios SQT/MT and ISO/MT for the area (approx. 450 km x 450 km) surrounding Zurich, Switzerland, and Hyytiälä, Finland, calculated for summer 2011 using the MEGAN biogenic emission model (Jiang et al., 2019)

3 H/C Probability density functions of CHO compounds

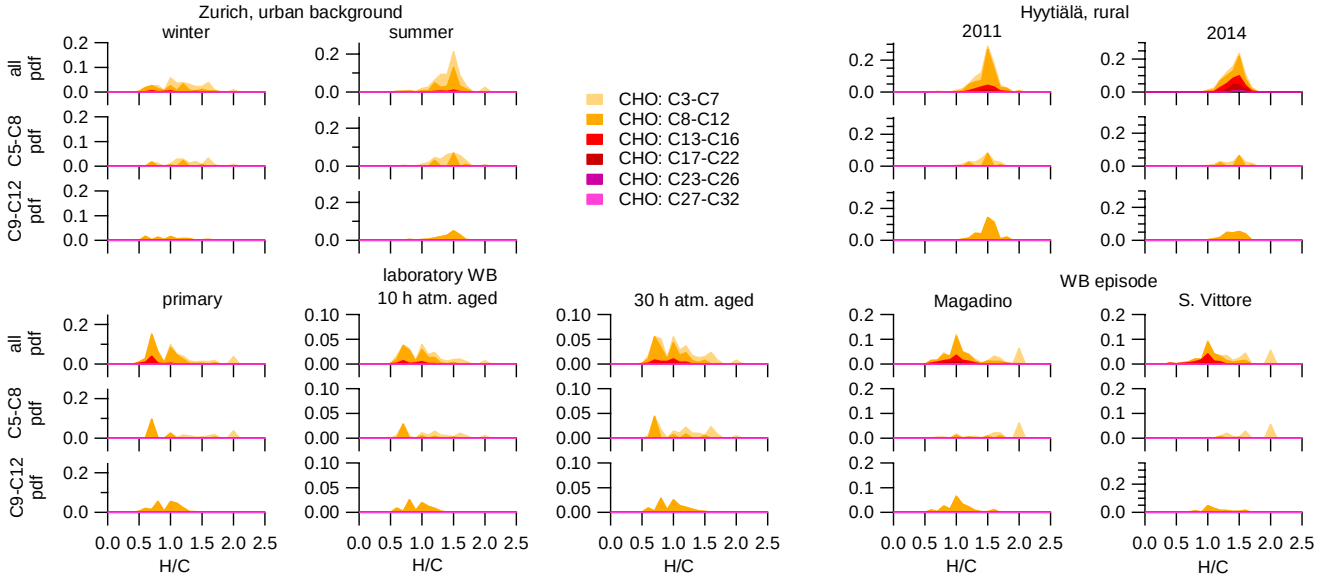

Figure S3: H/C probability density functions (pdf) for all CHO molecules (neutral composition based on (-)ESI-ultra-high resolution mass spectra), molecules with 5 to 8 carbons, respectively 9 and 12 carbon atoms for the ambient samples collected in Zurich, Magadino, S. Vittore, and wood burning smog chamber experiments. The area of the histograms is proportional to the percentage of the total signal explained in the respective site.

4 Van Krevelen diagrams color-coded with aromaticity for wood burning influenced samples

Van Krevelen diagrams of CHO compounds detected during wood burning smog chamber experiments and at alpine valley sites during wood burning episodes (color-coded with the aromaticity equivalent X_c, Fig S4).

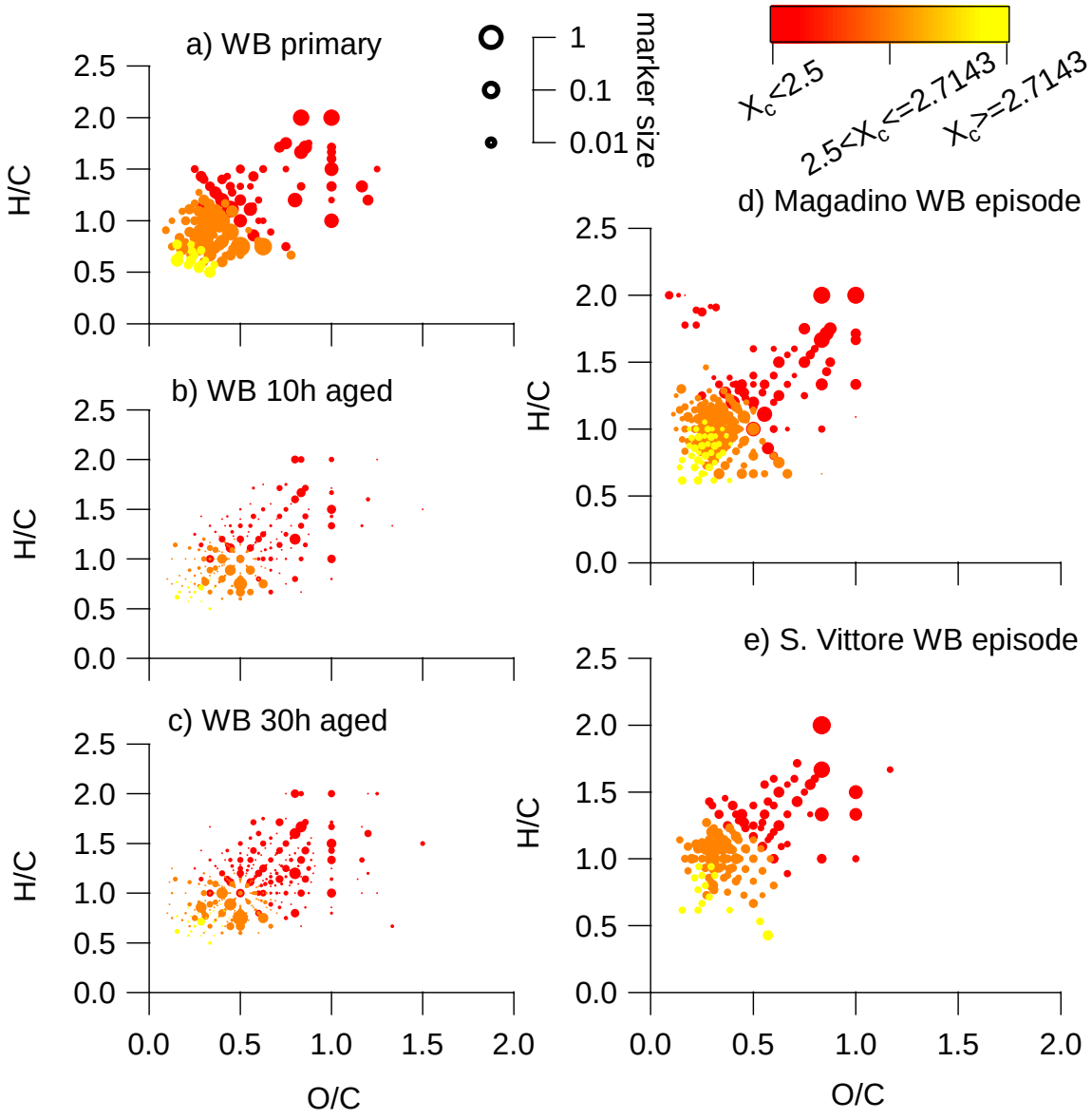

Figure S4: Van Krevelen diagrams of negative ion mode spectra (neutral composition) of smog chamber wood burning experiments (fresh emissions, after 10h of simulated atmospheric aging, and after 30h of simulated atmospheric aging) and wood burning episodes at the alpine valley sites Magadino and S. Vittore. Peaks are displayed as circles with their size reflecting log(intensity) and the color-code the aromaticity equivalent X_c (X_c <2.5 being non-aromatic, 2.5≥ X_c <2.7143 being aromatic, X_c ≥2.7143 being condensed aromatic).

5 Van Krevelen diagrams color-coded with aromaticity for Zurich

Van Krevelen diagrams of CHO compounds detected in Zurich (color-coded with the aromaticity equivalent X_c, Fig S5).

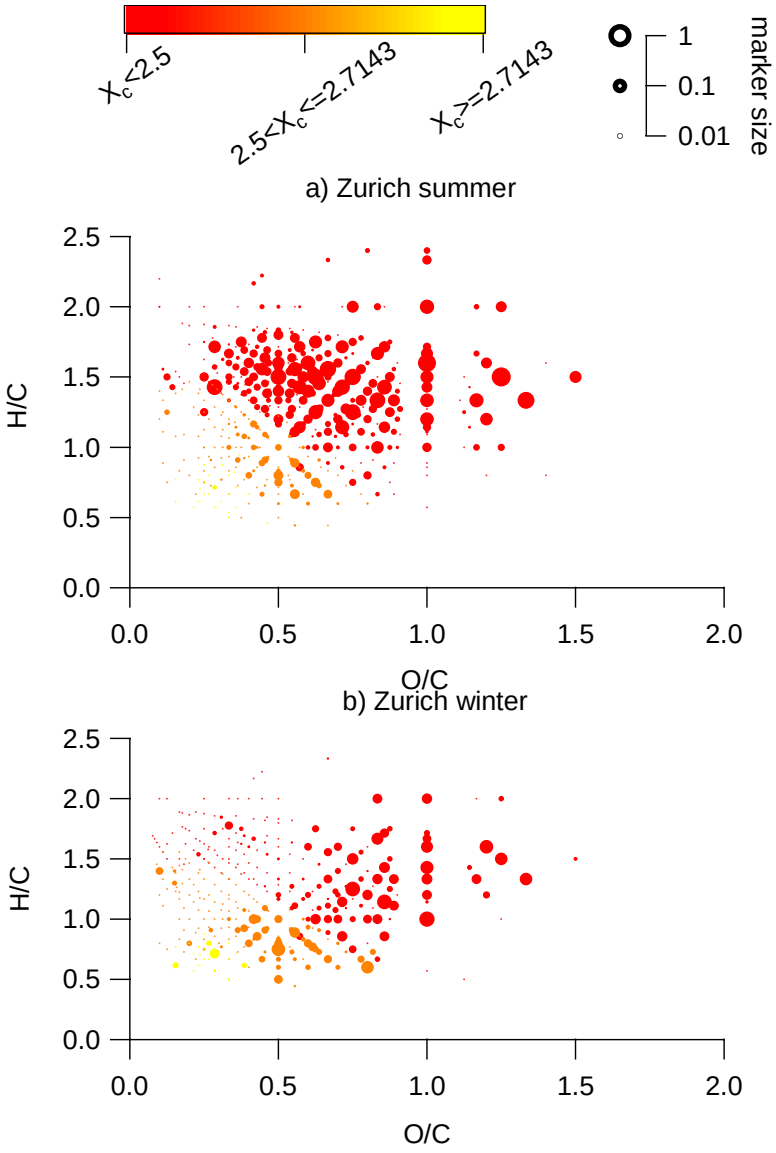

Figure S5: Van Krevelen diagrams of CHO compounds (neutral composition) of average summer (T>11°C, OA mass-weighted) and winter (T<6°C, OA mass-weighted) ultra-high-resolution mass spectra in the negative mode for the organic aerosol in PM10 sampled in Zurich during the year 2013 (weighted average with OA concentration from offline AMS analysis). Peaks are displayed as circles with their size reflecting log(intensity) and the color-code the aromaticity equivalent X_c (X_c <2.5 being non-aromatic, 2.5≥ X_c <2.7143 being aromatic, X_c ≥2.7143 being condensed aromatic).

6 Mass spectral signature separated by aromaticity

Spectra of only the CHO compounds for wood burning smog chamber experiments, wood burning episodes at alpine valley sites (Magadino, S. Vittore) and for Zurich during winter (color-coded with the aromaticity equivalent Xc, Fig S6).

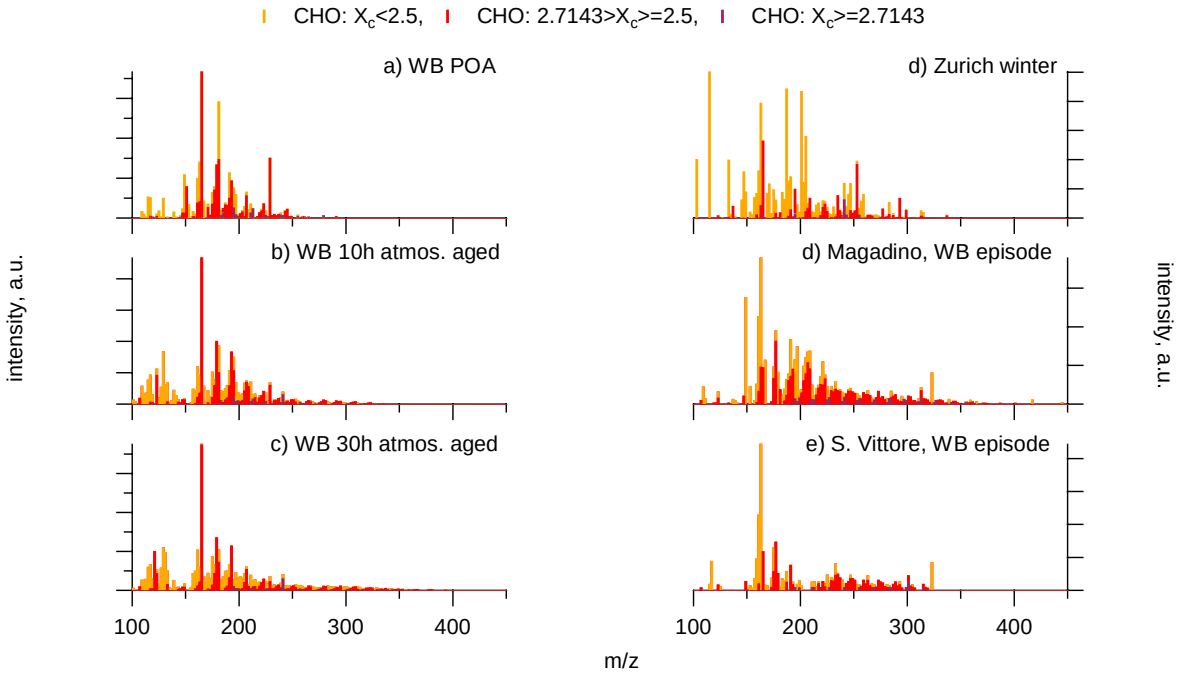

Figure S6: ultra-high-resolution mass spectra of CHO compounds integrated to unit-mass resolution of wood burning laboratory experiments (a: primary emissions, b: emissions 10 hours atmospheric aging, c: emissions 30 hours atmospheric aging), and from winter wood burning episodes at alpine valley sites (d: Magadino, e: S. Vittore). The signal at a nominal mass is separated by ion family (CHON, CHOS, CHONS, other) and the signal of CHO compounds by aromaticity (normal: X_c>2.5, aromatic: 2.5≤ X_c <2.7143, condensed aromatic: X_c ≥2.7143). Peak assignments of dominant ions of selected UMR peaks are labelled as neutral compounds.

7 Contributions of compound classes to the signal

The contribution of CHO, CHON, CHOS, and CHONS compounds varies as a function of the season and measurement location (Fig. S7).

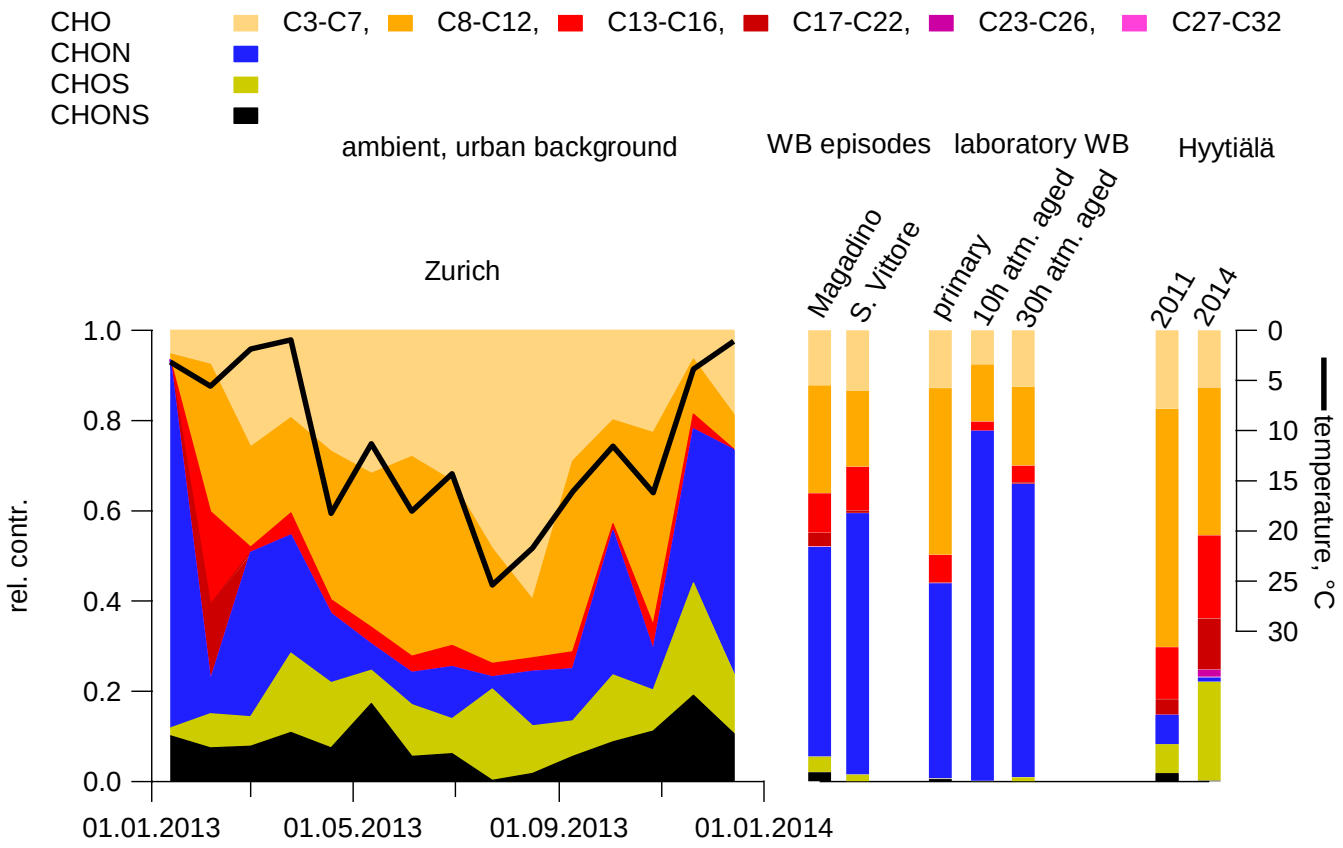

Figure S7: relative contributions of different compound classes to total signal.

8 Influence of instrumental settings

We investigated the possibility of artefacts induced by differences in vaporizer temperature by measuring 2 samples at the two used vaporizer temperatures (230°C-254°C). We found that differences induced by the temperature change were not statistically higher than our repeatability and were clearly lower than differences observed between samples. This suggests that temperature induced fragmentation artefacts are not a major driver of the observed chemical composition. The comparison between the two settings is shown in Figure S8.

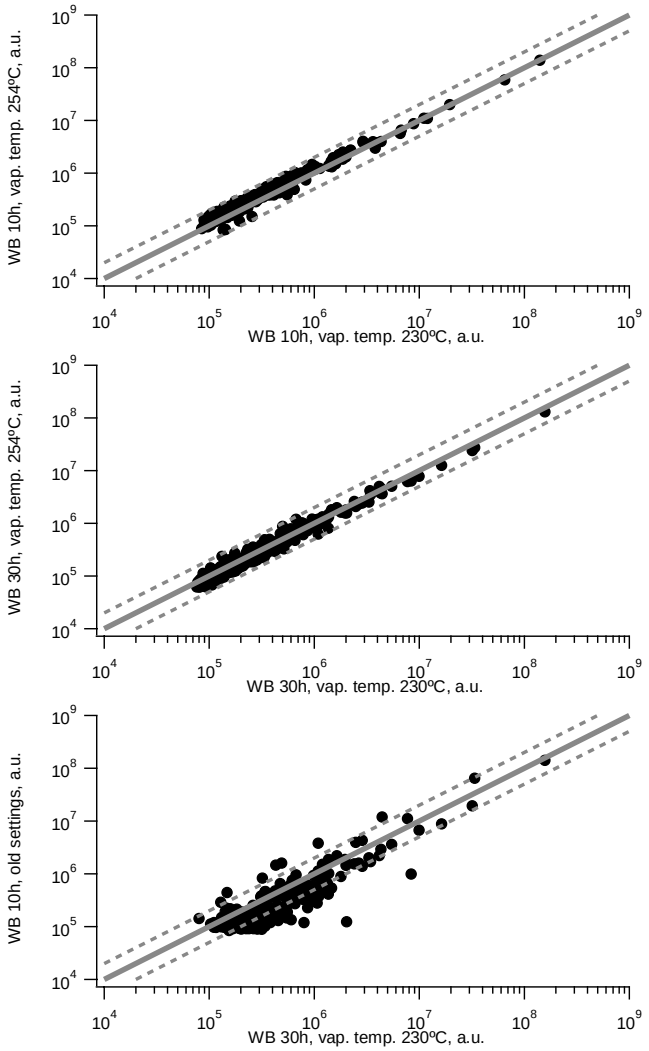

Figure S8: Comparison of mass spectra recorded with 2 different instrumental settings vaporizer temperature 230°C and 254°°C) for (a) a sample representing wood burning smoke (30h atmospherically aged) and (b) a sample representing wood burning smoke (10h) aged); (c) a comparison of the 2 samples measured with the same settings (vaporizer temperature 230°C). Measurements are displayed as black dots, 1:1 line as solid grey line, 1:2 and 2:1 line as strikethrough line.

9 Variability among replicate measurements

In order to estimate the relative error we performed replicate measurements of all samples (here computed as: $(x_{i,\max} - x_{i,\min})/x_{i,\text{avg}}$), with $x_{i,\max}$, $x_{i,\min}$, $x_{i,\text{avg}}$ being the maximum, minimum, and average peak (i) intensity measured for a respective sample. While the relative error varies considerably for a constant median peak intensity, overall typically the relative error ranges between 8 and 27%.

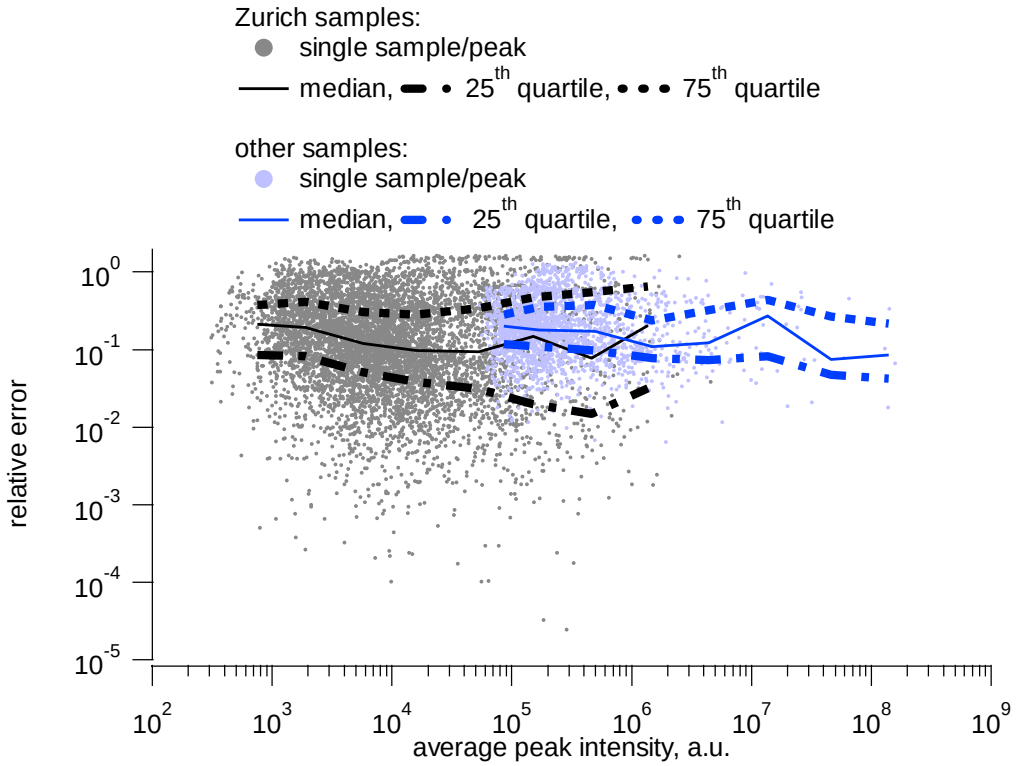

Figure S9: relative error as a function of the average signal intensity displayed for all samples and peaks.